$YBa_2Cu_3O_{7-\delta}$ Superconducting Films Prepared by Low Pressure Post-annealing

Lianhong Wang, Chong Liu and Jing Fan

State Key Laboratory of High-temperature Gas Dynamics, Institute of Mechanics, Chinese Academy of Sciences, Beijing 100190, China

Abstract. $YBa_2Cu_3O_{7-\delta}$ precursor films are deposited on 2″ $LaAlO_3$ wafer by the co-evaporation technique using Y, BaF_2 and Cu as evaporation sources. After deposition, the films are annealed at low-pressure atmosphere with the composition of oxygen and water vapour. Compared with the normal pressure annealing, it is shown that low pressure can greatly improve the superconducting properties of 2″ YBCO films with thickness larger than 500 nm, as the microcrack on films surface becomes unobservable the microwave surface resistance is greatly reduced. Furthermore, it is also revealed that the optimal processing window for making high quality superconducting YBCO films through ex-situ process is relatively small, therefore the ambient in annealing furnace is crucial important and should be precisely controlled.

Keywords: $YBa_2Cu_3O_{7-\delta}$, superconducting films, low pressure, post-annealing
PACS: 68.37.Hk, 68.37.Y, 68.55.J-, 68.55.jm, 74.25.nn, 74.72.-h, 74.78.-w, 81.15.Dj

INTRODUCTION

$YBa_2Cu_3O_{7-\delta}$ (YBCO) films are expected to achieve numerous applications in microwave systems because of low microwave surface resistance [1]. A number of methods including thermal co-evaporation, pulsed-laser deposition (PLD), sputtering, metal-organic deposition (MOD) and metal organic chemical vapor deposition (MOCVD) are currently used for the fabrication of YBCO films [2-7]. Actually, two types of sophisticated synthesis techniques based on thermal co-evaporation, i.e. the in-situ and ex-situ process, are most commonly utilized to prepare YBCO superconducting films. For ex-situ methods [8-9], the whole process can be divided into the deposition step and post-deposition annealing step. During deposition step, the electron guns are usually employed to heat the evaporation sources of Y and Cu, while the BaF_2 is evaporated by a well-designed thermal resistance heater. As the ($LaAlO_3$) wafer is rotating inside vacuum chamber, the deposition atoms/molecules of Y, Cu and BaF_2 can be mixed uniformly on the wafer with an approximate stoichiometric composition, and then the precursor films eligible for sequentially annealing is ready.

Post-annealing process is crucial for the ex-situ growth of YBCO superconducting films [10]. Through annealing, the deposited atoms reorganize themselves, the amorphous precursor films transform into single crystals with orthogonal lattice structure [11-12]. Without suitable annealing, the promising superconductive and magnetic properties can not be expected, and hence the quality of YBCO superconducting films strongly depends on the annealing parameters. Our previous experiments [13-14] indicate that good *c*-axis alignment, high critical current density J_c can be obtained on condition that the thickness of the YBCO films is less than 300 nm; however, when the thickness of YBCO films is larger than 500 nm especially for the films with large size, e.g. 2 inches in diameter (2″), the YBCO films may have porous structure with microcrack, and hence the superconducting properties will be deteriorated. Since atomistic reconstruction in the annealing processes is determined by a serial of chemical reactions, which is dominated by the transport of reactants. As the thickness of films increases, the transport of reactants might be blocked by thick YBCO precursor films [15-16], and consequently deteriorate the superconducting properties. In order to circumvent this, we reduce the total pressure in the annealing process with the consideration that it could enhance the transport of reactants and then improve the quality of YBCO films.

EXPERIMENTAL DETAILS

Figure 1 shows typical profile for the ex-situ process of YBCO films. The Y and Cu metals were evaporated using 10 kW e-beam guns and a custom 600 W thermal evaporation source was used to evaporate BaF_2. Precursor films were deposited on 2″ $LaAlO_3$ (100) wafer. Only films with composition ratios of Y: Ba: Cu of 1:2:3 with the

Proceedings of the 29th International Symposium on Rarefied Gas Dynamics
AIP Conf. Proc. 1628, 446-450 (2014); doi: 10.1063/1.4902627

deviation no larger than 10% are used in this study. Inductively coupled plasma atomic emission spectrometry (ICP-AES) was used to determine stoichiometries of precursor films in each deposition. After that, post annealing was sequentially performed in a quartz furnace. The total pressure (including H_2O pressure and oxygen pressure) in annealing process was less than 100 Torr within the temperature range from 720℃ to 780℃. For such low annealing pressure, it's difficult to control the partial pressure of H_2O precisely. In this study, the tunable diode laser absorption spectroscopy (TDLAS) is employed to monitor the partial pressure of H_2O. The experimental setup is illustrated in Fig. 2. With the help of TDLAS and other instruments, the annealing pressure as well as the composition of the ambient gas inside the quartz furnace can be well controlled, which guarantees the experimental repeatability for the optimization of the annealing parameters.

After annealing, the desired crystal structure and superconducting properties of YBCO films were verified by a series of testing methods. The phase purity and texture structure of 2″ YBCO films were examined by using X-ray diffraction (XRD); and the scanning electron microscopy (SEM) were employed to detect the homogeneity and microstructure of YBCO films. A Philips model XRG3100 diffractometer with Cu-Ka radiation was used to record

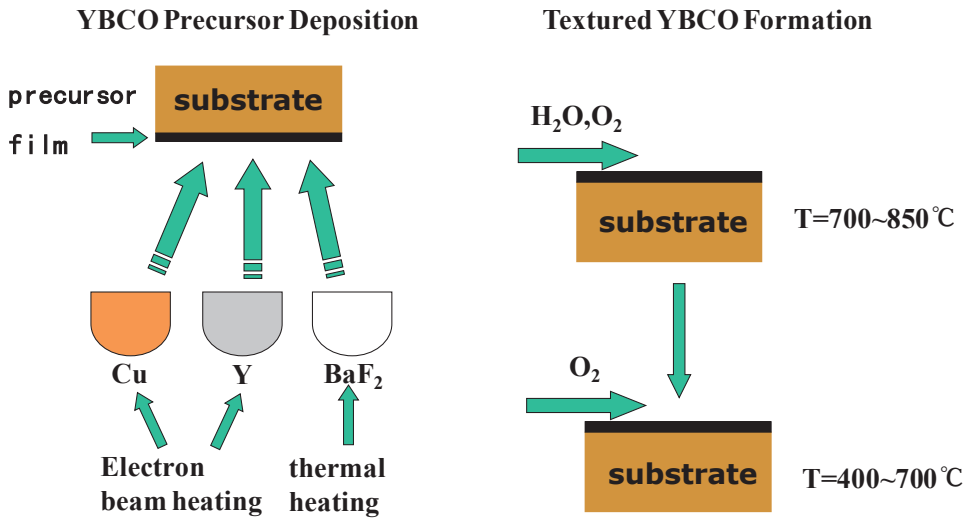

Figure 1. Typical profile for the ex-situ process of YBCO films.

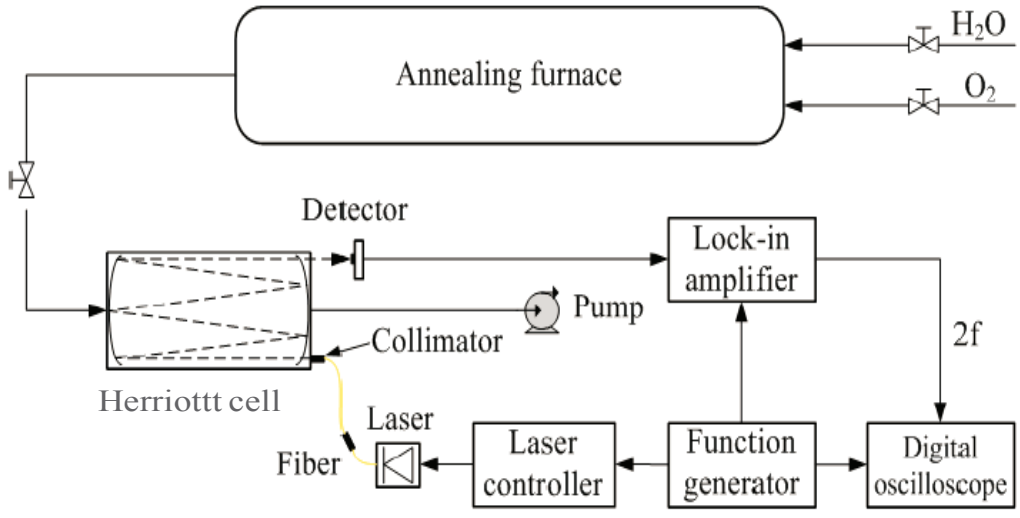

FIGURE 2. A schematic diagram of tunable diode laser absorption spectroscopy setup.

the θ-2θ XRD patterns. The texture analysis was performed using a Picker four-circle diffractometer. The microstructure analyses of these samples were performed using a Hitachi S-4100 field-emission SEM. The critical temperature T_c and critical current density J_c of the film samples were determined by the standard four-probe method. The microwave surface resistance (R_s) was measured at 12 GHz and 77 K in cylindrical resonant cavity. For the convenience of comparison, in the following discussion the values of R_s measured at 12 GHz are typically converted into the values at 10 GHz according to the well known relationship between the R_s and frequencies. The details of these tests are introduced and discussed in the following paragraphs.

RESULTS AND DISCUSSION

The structural quality of our fimls was examined by various XRD analyses: θ-2θ scans, rocking curves and (103) Φ-scans. Only YBCO (00*l*) reflections in the films is valid, as shown by θ-2θ scans in Fig. 3, which means that the YBCO crystals are well-developed in c-axis orientation.

We measured the rocking curves and Φ-scans to obtain evidence of epitaxial growth of YBCO on $LaAlO_3$ wafer. The rocking curves and Φ-scans are shown in Figs. 4 and 5. The (103) Φ-scans of the YBCO films illustrates four sharp peaks every 90 º, and full width at half maximum (FWHM) for all peaks is about 0.6 º, which reveals that the YBCO films have good in-plane textures. FWHM of the rocking curves is 0.67º, demonstrating the YBCO films have good out-plane textures. Figures 3-5 shows that YBCO films have good epitaxy on $LaAlO_3$ wafer.

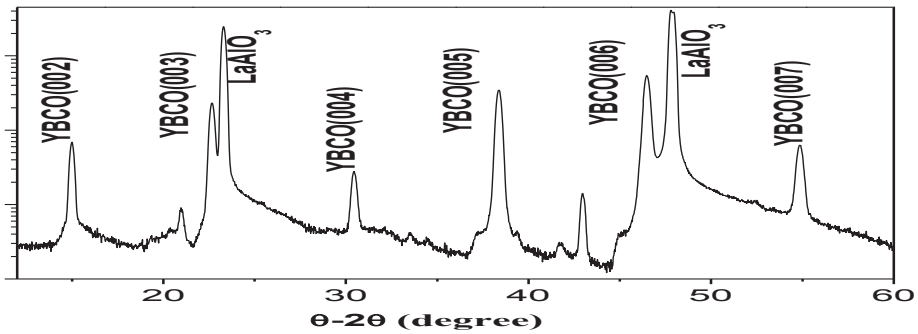

FIGURE 3. θ-2θ scans of the YBCO films.

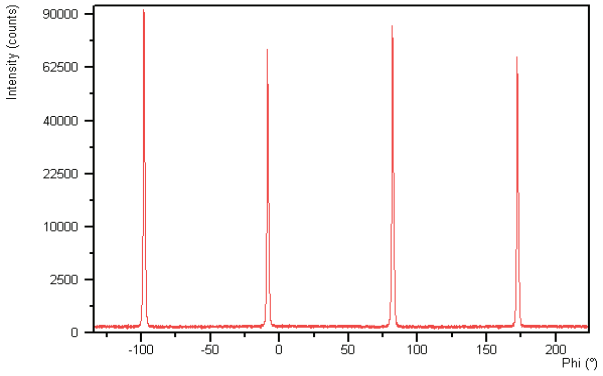

FIGURE 4. The (103) Φ-scans of YBCO films.

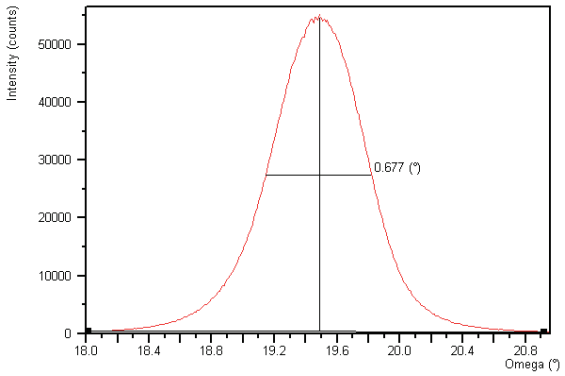

FIGURE 5. The rocking curves of YBCO films.

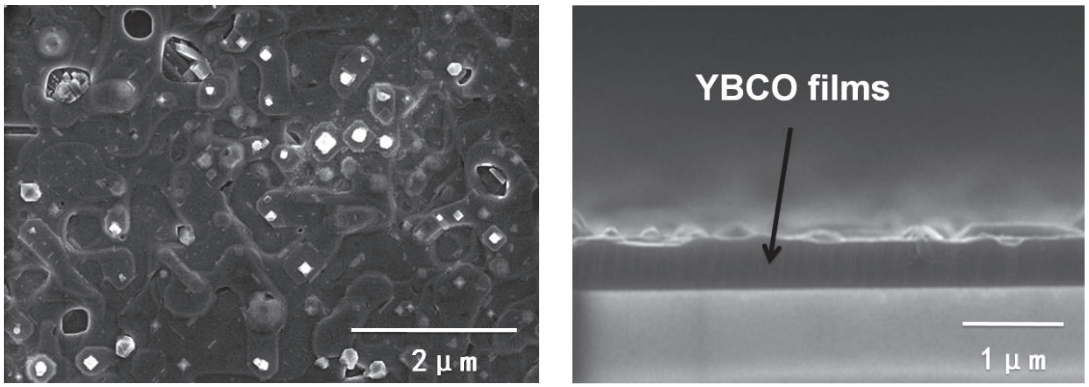

(a) (b)

FIGURE 6. SEM images of YBCO films. (a) Surface SEM (b) Cross Section SEM.

Table 1. Superconducting properties of 2″ YBCO films.

Superconducting critical temperature T_c	**Critical current density J_c (77 K, 0 T)**	**Surface resistance R_s (77 K，10 GHz）**
89 K	2 MA/cm^2	0.5 mΩ

Figure 6 (a) and (b) are SEM images of the surface and cross-section of YBCO films respectively. It is seen that the films have a crack-free surface and consist of c-axis-oriented grains, i.e., the grains in which the c-axis of the lattice is normal to the wafer surface. Moreover, the dense and crack-free cross-section has also been observed in Fig. 6(b). The above images and analysis confirm that the microcrack can be circumvented by reducing the annealing pressure.

As shown in Table 1, superconducting critical temperature (T_c) of YBCO films is about 89 K, and the critical current density J_c is around 2 MA cm^{-2} at 77 K in 0 T. The microwave surface resistance R_s measured in cylindrical resonant cavity reached as low as 0.5 mΩ at 10 GHz and 77 K. The result indicates that the YBCO films are suitable for microwave applications.

CONCLUSIONS

In conclusion, the post-deposition annealing is performed under low total pressure in this work for the fabrication of the 2″ YBCO thick films. After annealing the YBCO films were characterized by several measurement methods. The high epitaxy quality of YBCO films is confirmed by XRD results. The SEM results indicate that the YBCO films have crack-free surface. The improved superconducting performance indices, i.e. T_c is 89 K, J_c is about 2 MA/cm^{-2}, and R_s reaches as low as 0.5 mΩ at 10 GHz and 77 K, demonstrates that the films are suitable for microwave applications. The above results indicate that the properties of YBCO thick films can be greatly improved by reducing the anealling presure.

ACKNOWLEDGMENTS

We acknowledge technical assistance on absorption spectroscopy from Prof. Xilong Yu's group.

REFERENCES

1. Y. Ueno, N. Sakakibara, *J. Cryst. Growth* **222**, 697-700 (2001).
2. V. Boffa, T. Petrisor, U. Gambardella, et al, *IEEE T. Appl. Supercond.* **2**, 1189−1192 (1997).
3. F. Weiss F., J. P. Senateur, P. Chaudouet, et al, *Physica C* **372-376** (Supp 2), 652−655 (2002).
4. X. Z. Liu, B. W. Tao, A. Luo, et al, *Thin Solid Films* **l-2**, 225−228 (2001).
5. H. Kinder, P. Berberich, W. Prusseit et al, *Physica C* **282-287**, 107-110 (1997).
6. Y. Xu, A. Goyal, N.A. Rutter, et al, *J. Mater. Res.***3**, 677-681 (2003)
7. W. Wong-Ng, I. Levin, L. P. Cook, et al, *Appl. Phys. Letters* **88**, 102507 1-4 (2006).
8. M. Suenaga, *Physica C* **378–381**, 1045–1051(2002).
9. Y. Zhang, M. P. Paranthaman, R. Feenstra, et al, *IEEE T. Appl Supercond* **2**, 2659-2662 (2005).
10. V.F. Solovyov, H.J. Wiesmann, M. Suenaga, R. Feenstra, *Physica C* **309**, 269–274 (1998).
11. K. N. Tu, S. I. Park, and C. C. Tsuei, *Appl. Phys. Letters* **51**, 2158-2160 (1987).
12. C. Liu, J. Zhang, l. Wang, Y. Shu, et al, *Solid State Ionics* **232**, 123-128 (2013).
13. L. Wang, Y. Shu, and J. Fan, *Sci. China Technol. Sc.* **55** 2291-2294 (2012).
14. L. Wang, Y. Shu, and J. Fan, *Cryogenics Supercond.* **11**, 21−24 (2010).
15. T. Ohnishi, R. H. Hammond, and W. Jo, *J. Mater. Res.* **19***,* 977-981 (2004).
16. S. W. Chan, B. G. Bagley, L. H. Greene, et al, *Appl. Phys. Letters* **53**, 1443-1445 (1988).